Review in Advance first posted online on April 6, 2016. (Changes may still occur before final publication online and in print.)

Reagentless, Structure-Switching, Electrochemical Aptamer-Based Sensors

Lauren R. Schoukroun-Barnes, Florika C. Macazo, Brenda Gutierrez, Justine Lottermoser, Juan Liu, and Ryan J. White

Department of Chemistry and Biochemistry, University of Maryland, Baltimore County, Baltimore, Maryland 21250; email: rjwhite@umbc.edu

Annu. Rev. Anal. Chem. 2016. 9:15.1–15.19

The *Annual Review of Analytical Chemistry* is online at anchem.annualreviews.org

This article's doi:
10.1146/annurev-anchem-071015-041446

Keywords

biosensor, monolayers, binding affinity, charge transfer, functional nucleic acid

Abstract

The development of structure-switching, electrochemical, aptamer-based sensors over the past ~10 years has led to a variety of reagentless sensors capable of analytical detection in a range of sample matrices. The crux of this methodology is the coupling of target-induced conformation changes of a redox-labeled aptamer with electrochemical detection of the resulting altered charge transfer rate between the redox molecule and electrode surface. Using aptamer recognition expands the highly sensitive detection ability of electrochemistry to a range of previously inaccessible analytes. In this review, we focus on the methods of sensor fabrication and how sensor signaling is affected by fabrication parameters. We then discuss recent studies addressing the fundamentals of sensor signaling as well as quantitative characterization of the analytical performance of electrochemical aptamer-based sensors. Although the limits of detection of reported electrochemical aptamer-based sensors do not often reach that of gold-standard methods such as enzyme-linked immunosorbent assays, the operational convenience of the sensor platform enables exciting analytical applications that we address. Using illustrative examples, we highlight recent advances in the field that impact important areas of analytical chemistry. Finally, we discuss the challenges and prospects for this class of sensors.

1. INTRODUCTION

Electrochemical aptamer-based (E-AB) sensors: sensors fabricated with redox-labeled, structure-switching aptamers for reagentless sensing

Specificity: degree to which a biorecognition element is free from interference by other species, which is an intrinsic property of the aptamer sequence

Electrochemical aptamer-based (E-AB) sensors that utilize structure-switching nucleic acid aptamers have garnished the attention of researchers as a result of the specific, reagentless, and reversible analyte detection abilities of the sensor platform (e.g., see 1–10). Coupling the sensitivity of electrochemical methods with the specificity afforded by aptamer-based recognition opens electrochemical detection to a wide expanse of previously unattainable targets. There are a myriad of electrochemical detection schemes that utilize aptamers as a biorecognition element (11–13). In this review, we focus specifically on reagentless sensors that rely on structure-switching aptamers first introduced by Plaxco and coworkers (14) and the advantages provided by this detection scheme. This aptamer sensor architecture couples a target-induced change in aptamer conformation with a change in electron transfer ability between a distal-appended redox marker and an electrode surface (**Figure 1**) much like an electrochemical equivalent to fluorescent aptamer beacons (15).

Coupling electrochemical signaling to a change in aptamer conformation affords several advantages in analytical sensing. First, because the redox-active molecule is covalently linked to the nucleic acid aptamer, the change in electrochemical signal results solely from the target-induced conformation change of the aptamer. This signaling mechanism is less prone to signals arising from nonspecific interactions between matrix elements and the electrode surface (1, 4, 7, 8, 10, 16, 17). It is not uncommon to see a signal change resulting from nonspecific adsorption of proteins or other contaminants when a sensor is employed in a complex matrix; however, this signal typically equilibrates after ∼1 h, thus allowing for specific target quantification (1, 5, 8). Furthermore, because the redox-active reporter is covalently linked to the nucleic acid aptamer, the sensor is reagentless and reversible (5, 7, 14, 18). This allows sensor function without the addition of exogenous reagents, which enables real-time detection of changes in analyte concentration. These attributes render this class of sensor amenable to the development of field-deployable devices.

In this review, we focus on the fabrication and design of E-AB sensors and the parameters employed during these processes that affect analytical sensor performance. In addition, we emphasize several works that discuss the fundamentals of the electrochemical signaling observed with this class of sensors and provide a quantitative framework for evaluating sensor performance. We then highlight several illustrative examples and recent advances that take advantage of the unique

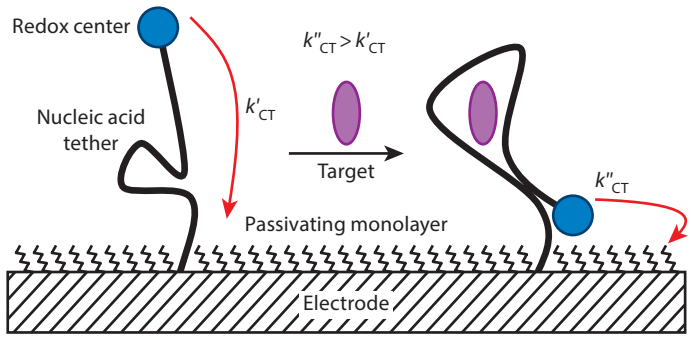

Figure 1

Reagentless, structure-switching, aptamer-based sensors employ DNA or RNA aptamers for the specific detection of analytes. To support reagentless sensing, the redox-labeled aptamer undergoes a flexibility and/or conformation change upon target binding that alters the charge transfer rate (k_{CT}) between a redox reporter and electrode surface. This change in charge transfer rate can be readily measured using a variety of different voltammetric methods.

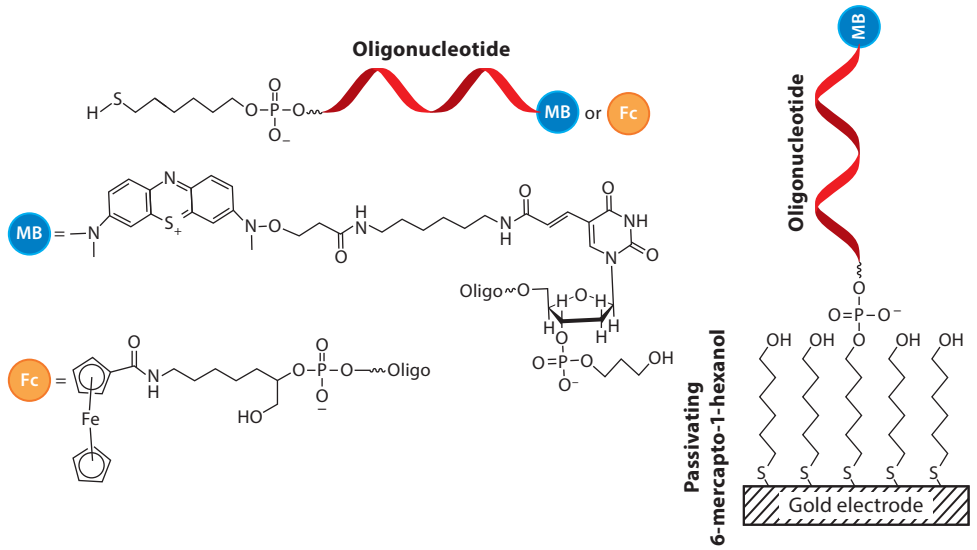

Figure 2

Electrochemical aptamer-based sensors comprise mixed monolayers of both a sensing aptamer, labeled at the distal end with a redox-active molecule, and a diluent or spacer thiol on the surface of a gold electrode. Typical redox marker linkages are either directly to the 3′-phosphate as shown in the Fc example or through a 3′-modified thymidine as indicated in the MB example. The most prevalent surface chemistries utilized in the literature include a six-carbon thiol linker at the 5′-phosphate group and 6-mercapto-1-hexanol as the spacer molecule.

attributes of structure-switching sensors, including some promising alternative strategies using structure-switching aptamers. Finally, we discuss some of the challenges that impede the progress of E-AB-type sensors. Despite these challenges, we believe that this class of reagentless and reversible detection shows great analytical promise in the fields of chemical, clinical, biomedical, and environmental sensors.

2. E-AB SENSOR FABRICATION PARAMETERS

2.1. Sensing Self-Assembled Monolayer Chemistry

The fabrication of E-AB sensors is a relatively straightforward process; however, there are a variety of parameters that can affect the signaling and analytical performance of the resulting sensor. A typical gold electrode surface comprises a mixed monolayer of a thiol-modified nucleic acid and a diluent thiol spacer (**Figure 2**). The most often used spacer is an alcohol-terminated, six-carbon alkane thiol (6-mercapto-1-hexanol). Early studies by Herne & Tarlov (19) demonstrated that the deposition of thiolated DNA followed by 6-mercapto-1-hexanol as a diluent lifts any nonspecifically bound DNA and enables reproducible control over DNA packing density. Using this backfill method, these authors established that the packing density of the DNA on the surface affects the hybridization efficiency of complementary DNA, demonstrating the importance of this parameter on sensor performance. Packing density is likewise an important factor when considering the performance of aptamer-based sensors, as discussed in detail below. More recently, Josephs & Ye (20) published a study on mixed monolayer formation using an insertion method in which the passivating monolayer is deposited followed by the deposition of thiolated DNA.

Binding affinity: the dissociation constant (K_d) is often used as a quantitative benchmark to describe the performance of E-AB sensors

Using atomic force microscopy, Josephs & Ye (20) observed that the insertion method resulted in reproducibly dispersed monolayer surfaces in contrast to the aggregates of DNA observed using the backfill method. The nature of the sensing monolayer is now an important aspect to consider when fabricating sensors (21).

The chemistry of the passivating monolayer represents a compromise between sensor signaling and stability (2, 22). Increasing the number of carbons in an alkane thiol chain results in improved monolayer packing as a result of increased van der Waals interactions between neighboring thiols (23). Consequently, increasing thiol length also increases monolayer thickness, which results in a larger separation distance between the redox molecule and electrode surface. An increased separation distance results in a larger tunneling barrier (23), compromising the magnitude of measurable faradaic current. Lai et al. (22) explored the difference in stability and signaling of an electrochemical DNA-based sensor employing either a 6-carbon or 11-carbon passivating thiol. They demonstrated that sensors fabricated with an 11-carbon thiol exhibited significantly improved lifetimes while maintaining an appreciable single-to-noise ratio. Although these studies do not employ aptamer sequences, they do use structure-switching nucleic acids to detect complementary nucleic acid, and they serve as a reasonable analog to E-AB sensors. It should also be noted that in these studies, the number of carbons in the alkane thiol linker at the 5′-end of the DNA matched that of the passivating layer.

In addition to thiol length, the charge on the exposed terminus of the passivating monolayer also affects the signaling abilities of structure-switching nucleic acid sensors. For example, Ricci et al. (24) demonstrated that sensor performance improved for both positively (amine-terminated thiols) and negatively charged (sulfonic acid–terminated thiols) monolayers. Specifically, both monolayers improved the maximum signal (sensor signal observed at saturating target concentrations) for DNA-based sensors when compared with the sensors fabricated with 6-mercapto-1-hexanol (neutral). The origin of these signal improvements, however, is unclear, and 6-mercapto-1-hexanol remains the most widely used passivating thiol.

2.2. Aptamer Packing Density

As suggested in the initial study by Herne & Tarlov (19), the packing density of the nucleic acid aptamer (aptamers/cm^2) on an E-AB sensor surface is a readily controllable parameter to optimize sensor performance. Aptamer packing density is controlled by the concentration of thiolated aptamer, incubation time, and temperature employed during monolayer formation. Values reported for aptamer packing density range from $\sim 10^{11}$ to 10^{13} aptamers/cm^2 (2, 25). These values represent $\leq$10% of the maximum packing density of $\sim 9 \times 10^{13}$ molecules/cm^2 assuming a 0.7-nm cross-sectional radius for fully extended, single-stranded DNA (26). The optimal packing density for a given aptamer sequence, as determined by sensor performance, is dependent on the aptamer geometry (tertiary structure) as well as the size and structure of the target analyte (2). In general, steric interactions between neighboring aptamers can inhibit target accessibility and aptamer folding at high aptamer packing densities. The latter can significantly alter the observed binding affinity (K_d) of the sensor (2, 25). When aptamer packing densities become too low, the number of aptamers on the surface may not produce an appreciable faradaic signal above the background.

2.3. Covalently Attached Redox Molecule

The majority of E-AB sensors employ the reversible redox couples methylene blue (1, 10, 27, 28) or ferrocene (9, 10, 16) as the redox-active tag, and each molecule offers different advantages and disadvantages (10, 16). The covalent coupling of methylene blue is typically achieved by reacting a 3′-amine-terminated nucleic acid with *N*-hydroxysuccinimide ester-activated

methylene blue (29). Ferrocene can be coupled using similar chemistry with a ferrocene carboxylic acid *N*-hydroxysuccinimide ester and has been done both pre- and post-monolayer formation. Ferapontova et al. (16) demonstrated that the latter coupling procedure provides better coupling efficiency of the redox marker.

The convenience of reversible electrochemical behavior and standard conjugation chemistry makes both molecules ideal candidates for use as signaling moieties. Methylene blue undergoes a reversible two-electron, one-proton reduction (29) and has seen the most widespread use. However, the redox reaction is sensitive to changes in pH; thus, care must be taken when working in conditions where pH is unknown or varies. Conversely, ferrocene undergoes a reversible, one-electron oxidation to form ferrocenium. However, ferrocenium is prone to nucleophilic attack even by mild nucleophiles like chloride, which ultimately can displace the molecule from the nucleic acid (30). This limits the utility of ferrocene labels in physiologically relevant solutions. This limitation can be avoided by using buffers that do not contain strong nucleophiles (16, 31, 32). Ferapontova & Gothelf (29) demonstrated that the use of ferrocene as a redox label in physiological matrices is problematic. Specifically, their study demonstrated that the positive potential at which ferrocene is oxidized with respect to the point of zero charge on the electrode surface induces nonspecific protein adhesion (10, 29).

The use of these reversible redox couples offers the advantage of reagentless and reusable sensor signaling. More specifically, because aptamer-target binding and the electrochemistry of the redox tags are reversible, E-AB sensors report real-time changes in the concentration of target analyte. However, the sensor response time can be limited by aptamer binding kinetics. Reports indicate that association rate constants range from $\sim 10^3$ to 10^5 1/Ms and dissociation rates range between $\sim 10^{-2}$ and 10^{-3} s^{-1} for small-molecule binding (33, 34). The downside to these common redox markers is the finite amount of charge available for measurement. There is a finite number of molecules on the surface, and each molecule provides at most either one or two electrons worth of charge. This ultimately can limit the sensitivity and limit of detection of the E-AB sensor. As we discuss below, the ability to introduce an amplification strategy that maintains the reagentless nature of the sensor could prove to be a major advancement in the development of E-AB sensors and ultimately push limits of detection down toward levels seen with enzyme-linked immunosorbent assays.

Several other oligonucleotide-bound redox markers have been employed, such as iron oxide particles (32) and anthraquinones (35), but have seen less widespread use. Introduction of new redox reporters with different standard reduction potentials enables multiplexed detection. For example, Revzin and coworkers (35) recently developed sensors with a mixed monolayer of methylene blue–modified tumor necrosis factor alpha aptamers and anthraquinone-modified interferon gamma aptamers to detect both targets simultaneously using the same electrode surface (**Figure 3**). Their study demonstrated several compelling features of E-AB sensors, including the selective detection abilities of electrochemical detection, the specificity of aptamer-target interactions, and the ability to function in complex media (e.g., cell-culture media).

3. FUNDAMENTALS OF SENSOR SIGNALING

3.1. The Electrochemistry of E-AB Sensors

The packing density of nucleic acids on a typical E-AB sensor surface is such that the dynamic motion of the biopolymer chain becomes important in determining the charge transfer rate between the redox molecule and the electrode surface. This dependence is the basis for signaling in structure-switching E-AB sensors.

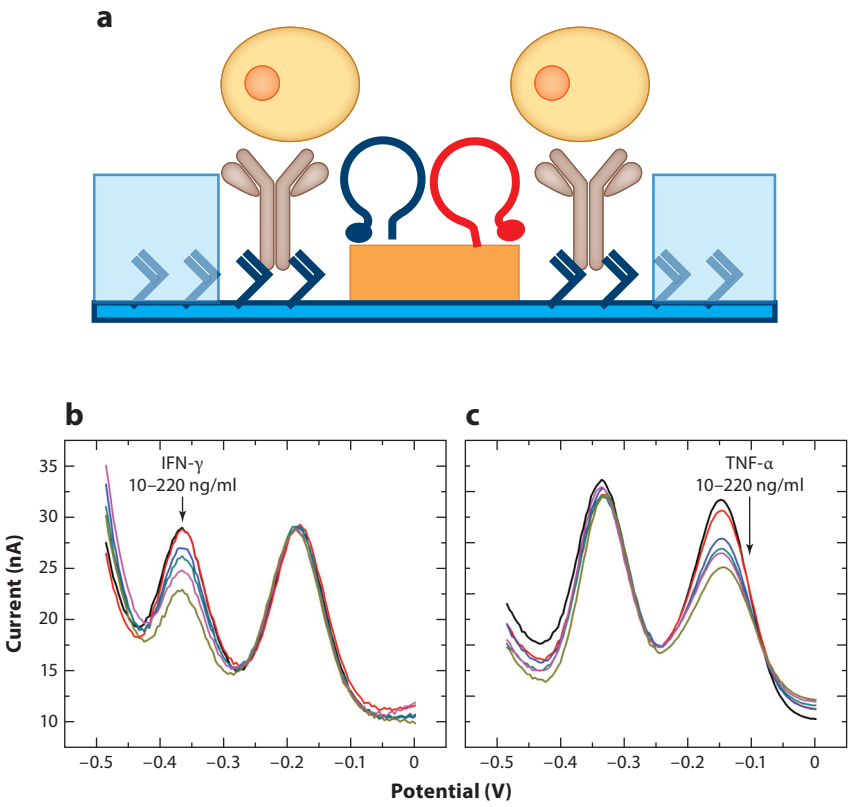

Figure 3

The use of multiple aptamers and redox reporters enables the simultaneous detection of multiple analytes (*a*), highlighting the specificity of aptamer recognition and the selectivity of electrochemical detection. The difference in the standard reduction potential of methylene blue (−0.15 V versus Ag/AgCl) (*b*,*c*) and anthraquinone (−0.37 V versus Ag/AgCl) is used for simultaneous multiplexed detection of various cytokines released from various cell types using the same electrode. Specifically, the presence of of IFN-γ is signaled via changes in the peak current corresponding to the reduction of anthraquinone (*b*) while the presence of TNF-α is signaled via changes in the peak current corresponding to the reduction of methylene blue (*c*). Adapted with permission from Reference 35. Copyright 2015, Elsevier. Abbreviations: IFN, interferon; TNF, tumor necrosis factor.

There have been several reports of quantitative models to describe the dynamic motion of end-grafted DNA on an electrode surface (36–41). Several of these, including a model we recently developed, use the electrochemical response of the tethered redox molecules to estimate an apparent diffusion coefficient for the tethered redox marker as a proxy for the motion of short nucleic acid strands (38–41). This measure is achieved by comparing the measured faradaic current at varying voltammetric scan rates. Using redox-labeled DNA, Moiroux and coworkers (40) reported that the electrochemical reaction exhibits Nernstian behavior at slow scan rates, as indicated by symmetrical cathodic and anodic peaks and little-to-no peak separation. This observation suggests that the experimental timescale at slow scan rates allows all the attached redox molecules to reach the electrode surface and transfer electrons. The authors used the area under the cathodic/anodic peak in this voltammetric regime to quantify the amount of nucleic acid on the surface. This measurement represents a direct, quantitative method for characterizing aptamer surface coverage.

It is unclear why this method is not used more commonly in the field. Typically, the preferred method is to indirectly measure the charge consumed from the electrochemical reduction of nucleic acid–associated $Ru(NH_3)^{6+}$, as first described by Tarlov and coworkers (42) to quantify unlabeled DNA on a surface. This method, however, was originally used on electrode-grafted nucleic acids without covalently attached redox molecules.

Selectivity: degree to which the method is free from interference by other species in a complex sample matrix

Much like a thin-layer electrochemical cell, as the experimental timescale is shortened by increasing the voltammetric scan rate, a diffusion-dependent electrochemical response emerges for nucleic acid–tethered redox molecules (similar to those used in E-AB sensors) (38–41). Coupling this experimental observation with random-walk simulations, we recently reported a quantitative metric for estimating an apparent diffusion coefficient of a flexibly tethered redox molecule at the distal end of a surface-bound nucleic acid (38). Typically, in thin-layer electrochemistry, the electrochemical reaction follows Nernstian behavior when the cell thickness (L, analogous to nucleic acid tether length) is much less than the diffusion layer thickness [$(2Dt)^{1/2}$] as determined by the scan rate (ν, V/s) and diffusion coefficient (D, cm^2/s) of the molecule. We found that this criterion is met when the diffusion layer thickness is less than 10 times the tether length: $10L \leq (2Dt)^{1/2}$. Using this criteria, we estimated diffusion coefficients of $\sim 7 \times 10^{-11}$ cm^2/s for redox molecules tethered to unstructured poly-thymine linkers. These estimated diffusion coefficients are similar to those reported by Moiroux and coworkers (40) and Ferapontova and coworkers (39).

The dependence of sensor signaling on the voltammetric scan rate leads the way to voltammetric interrogation methodology optimization. E-AB sensors function on the basis of changes to the charge transfer rate as a result of target-induced conformation changes that alter the structure and the apparent diffusion coefficient of the appended redox molecule. Each state—target bound and unbound—has different charge transfer rates, which are likely limited by aptamer flexibility, allowing for quantitative determination of the presence of the target (**Figure 1**). This observation can be used to further optimize sensor signaling as we discuss in detail below.

3.2. Quantitative Binding Curves and Analytical Figures of Merit

Quantifying the analytical response of E-AB sensors is necessary for benchmark comparison with existing sensing techniques and strategies. As mentioned above, there are several factors in the fabrication and analysis of E-AB sensors that can dramatically affect sensor performance. As a baseline, there are several core analytical figures of merit that can be used to describe the performance of these sensors, including sensitivity and limit of detection. Often reports on the binding affinity, specificity, and selectivity are also used for benchmarking. For clarity, specificity is defined as the degree to which the biorecognition element is free from interference by other species, which is an intrinsic property of the aptamer sequence. Selectivity is defined by the degree to which the method (i.e., electrochemical detection) is free from interference by other species in a complex sample matrix.

When tested at the limit of saturating concentrations, equilibrated E-AB sensor response follows a Langmuir-like binding isotherm. For a given electrode surface, there is a finite number of binding sites (aptamers) and a target concentration at which all binding sites are occupied. This type of binding follows the Langmuir isotherm model with several assumptions, including that target binding to one aptamer does not affect target binding to a neighboring aptamer or that the binding sites are noninteracting. This, of course, may not hold true at high packing densities. Moreover, the assumption is made that target binding does not appreciably alter the free target concentration in bulk solution. Though this is generally true, when working with low concentration and small volumes, this can become problematic (43). Starting with an equilibrium expression for the target (L) to bind a receptor aptamer (R) and using the aforementioned assumptions, the fraction of

occupied sites (β) can be written as

$$\beta = \frac{K_a[L]}{1 + K_a[L]}$$

where K_a and $[L]$ are the association constant ($[R{:}L]/[R][L]$) and target concentration, respectively (21). Rewriting β in terms of K_d (the dissociation constant or binding affinity) and the sensor signal, the expression for sensor signaling becomes

$$\frac{S}{S_{max}} = \frac{[L]}{K_d + [L]} \text{ and } \frac{S}{S_{max}} = \beta$$

where S and $S_{\max}$ (i.e., peak current) are the sensor signal at a given concentration and sensor signal at saturating concentrations, respectively. When binding data are fit to this model, the binding affinity is only an apparent affinity and does not necessarily represent the intrinsic binding affinity between the aptamer and target analyte. This apparent affinity can change according to the sensitivity of the sensor device, which can be significantly altered by changing the voltammetric interrogation frequency or scan rate, or the aptamer geometry as discussed below in more detail.

The Langmuir-type isotherm described above can be expanded by using multiple aptamers that bind the same target but with different affinities. We recently reported that a bi-Langmuir isotherm accurately predicts the E-AB sensor response as a result of the ratio of the different aptamers employed on the sensor surface, the individual observed binding affinities, and S and $S_{\max}$ (**Figure 4**) (44). Creating heterogeneously covered sensor surfaces with multiple aptamers represents a method to rationally tune the sensitivity and dynamic range of the resulting sensor.

3.3. Tuning Analytical Figures of Merit

A compelling aspect of E-AB sensors is the ability to tune the analytical figures of merit. As mentioned above, sensor fabrication parameters can affect the analytical performance of the resulting aptamer sensor. However, control over performance is typically minimal in magnitude. Fortunately, there are a variety of other methods to optimize sensor response that have large effects on analytical performance.

3.3.1. Voltammetric methods of interrogation. Given that the motional dynamics and change in the dynamics of the sensing aptamer are important factors in signaling, it is not surprising that the timescale of the voltammetric interrogation is an important parameter in sensor function. Cyclic, alternating-current (ACV), square-wave (SWV), and differential-pulse voltammetry are all suitable methods for monitoring aptamer conformation change and the resulting change in charge transfer rates. The latter three are particularly well suited for monitoring surface-confined reactions, as they reduce nonfaradaic background charging currents. The experimental timescale in each method is dictated by the scan rate or frequency used and can have profound effects on signaling—especially in the differential technique of SWV.

The frequency of the excitation potential waveform employed in ACV, SWV, and differential-pulse voltammetry affects sensor sensitivity, signal change magnitude, polarity, and observed binding affinity (2, 28, 45, 46). Signal polarity refers to either the increase (signal-on sensor) or decrease (signal-off sensor) in faradaic current upon target addition. In the specific case of SWV, the magnitude of signal change at saturating conditions and the signal polarity of a given sensor can be dramatically altered (2, 28, 45, 46). The dependence of sensor performance on the square-wave frequency employed is attributed to the timescale of the voltammetric measurement (frequency) with respect to differences in the apparent rate between the target-bound and -unbound states

ACV: alternating-current voltammetry

Square-wave voltammetry (SWV): a differential pulsed potential voltammetry commonly used to interrogate E-AB sensor surfaces

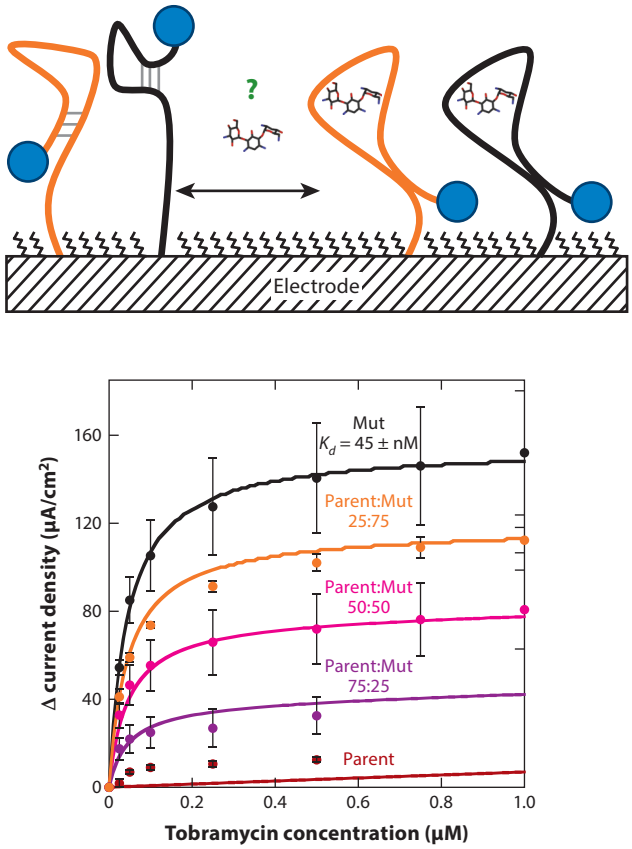

Figure 4

Use of multiple aptamers with different binding affinities on the same surface enables tunable sensor response with respect to the aptamer ratio used. The ratio of the aptamers on the sensor surface dictates the sensor response and alters the maximum signal change observed at saturating target concentrations. The sensor response of heterogeneously coated surfaces follow a bi-Langmuir binding isotherm. Figure adapted with permission from Reference 44. Copyright 2015, American Chemical Society. Abbreviation: Mut, mutated aptamer.

(**Figure 5**) (28, 46). In SWV, the current is sampled near the end of each square-wave pulse; thus, the magnitude of current measured is related to the rate of the charge transfer reaction. Because the target-bound and -unbound states have different charge transfer rates, the magnitude of current measured for a fixed pulse width (frequency) is different. For example, as an approximation, a sensor in the unbound state with a charge transfer rate of 100 s^{-1} gives a higher measurable current using a frequency of 100 Hz than that of the bound state with a charge transfer rate of 6 s^{-1} (45). Conversely, if using a square-wave frequency of 5 Hz, the sensor in the bound state gives a larger measurable current than that of the unbound state. This leads to a signaling polarity switch from a signal-on to a signal off-sensor. Furthermore, maximizing the difference in measured current between the two states enables tuning of the sensor sensitivity. The interrogation frequency can be optimized for a given aptamer geometry. White et al. (2) and Ricci et al. (46), respectively, have shown the frequency dependency of sensor signaling abilities for E-AB sensors employing ACV and for E-DNA sensors employing ACV.

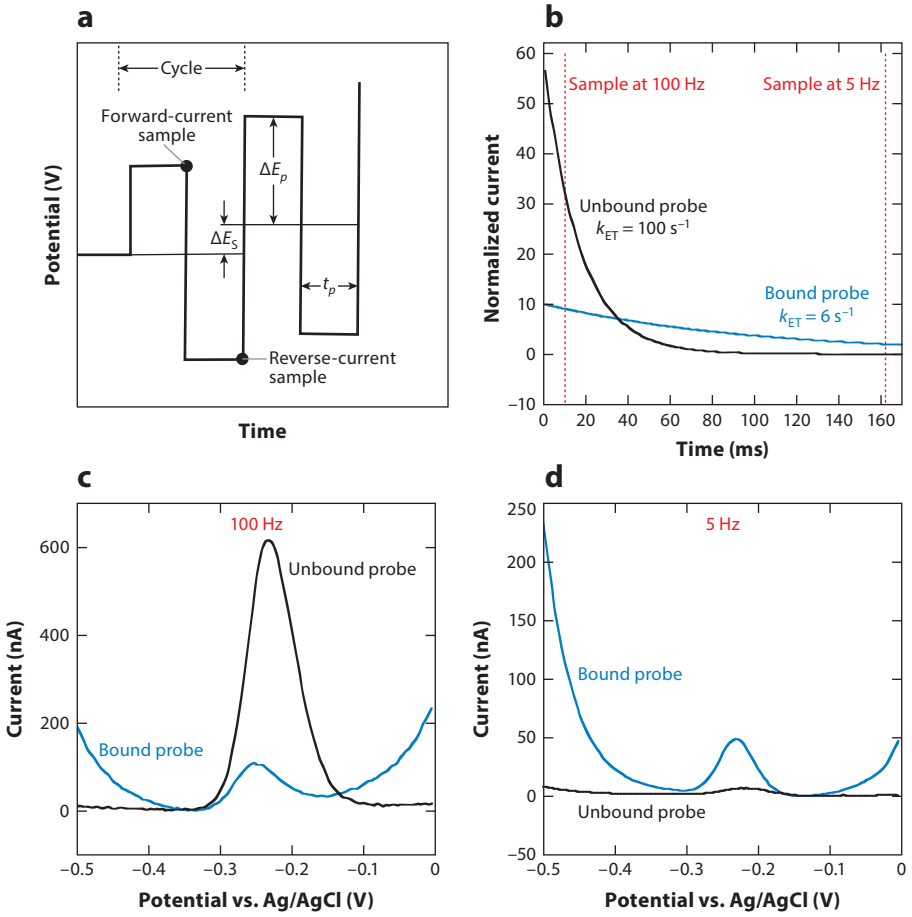

Figure 5

Electrochemical aptamer-based sensor signaling is dependent on the nature of the voltammetric interrogation methodology employed. A compelling demonstration of this phenomenon is seen when using the differential voltammetric technique of square-wave voltammetry. White & Plaxco (45) demonstrated that sensor sensitivity and signaling polarity are controlled via the frequency of the square-wave potential waveform (*a*) used during voltammetric interrogation. Specifically, because sensor measurements compare the charge transfer rate in the bound and unbound state (*b*), each state can provide more faradaic current than the other depending on the width of each pulse in the potential waveform. At high frequencies, the faster charge transfer process provides more current. Conversely, at low frequencies, the slower charge transfer rate provides more current. This observation results in a switch in signaling polarity—from signal off to signal on—in sensor performance (*c*,*d*). Furthermore, maximizing the difference in current observed in each state leads to improvements in sensitivity. Figure adapted with permission from Reference 45. Copyright 2010, American Chemical Society.

3.3.2. Designing aptamer conformation for sensor signaling. Structure-switching aptamer-based sensors rely on a target-induced conformation change in the electrode-bound aptamer. The difference in charge transfer rate between the target-free state and the target-bound state is important in determining the signaling abilities of E-AB sensors. Unfortunately, current aptamer selection strategies do no select for functionality beyond target binding (i.e., there is no selection pressure for structure-switching aptamer). However, the base-pair programming language of

nucleic acids along with the aid of secondary structure prediction software [Mfold (47, 48)] enable the design of altered aptamer sequences to support reagentless electrochemical signaling (3, 18, 28, 45, 49–52).

Beyond creating aptamer sequences to support reagentless signaling, altering the aptamer sequence to modify the magnitude of the conformation change can have dramatic effects on the analytical performance of E-AB sensors. There are several strategies for creating alternative aptamer structures. Typical strategies include the destabilization of any secondary structure, generation of alternative folds of the aptamer, and introduction of the aptamer into a scaffold (3, 28, 45, 49, 52). Design can be further aided through the use of solution-phase three-dimensional structures of aptamer-target complexes. For example, we recently published a report that utilized a combination of secondary structure predictions and the nuclear magnetic resonance (NMR) structure of the aminoglycoside-binding RNA aptamer (53) to rationally design sequences to undergo larger conformation changes in the presence of tobramycin (28, 54). The NMR structure of the aptamer enabled careful conservation of nucleotides and portions of the RNA backbone postulated to bind tobramycin to maintain a specific binding ability (28). The aptamer sequence was altered outside of the binding site by removing base pairs to destabilize the secondary structure in the unbound state. Disrupting the stem-loop secondary structure of the parent aptamer forced the aptamer to undergo a larger conformation change upon target addition, significantly improving E-AB sensor sensitivity (28). Interestingly, given the similarities between the target-bound structure and the predicted secondary structure, it was surprising to find an improvement in the observed binding affinity of all new constructs. This observation indicates that the reported affinity for E-AB sensors is convoluted by the amount of signal the sensor can produce and is not necessarily a direct indication of the intrinsic binding affinity. We are currently investigating this observation to determine a quantitative relationship between signal and apparent affinity. As an alternative strategy, Bonham and coworkers (52) recently published a potentially universal approach to create reagentless structure-switching E-AB sensors by incorporating an aptamer sequence into a DNA scaffold. Their approach divides the aptamer into sections and incorporates each fragment into a structure-switching DNA scaffold. They demonstrated the universality of their approach by developing E-AB sensors using a ricin-binding and botulism toxin–binding aptamer. As a final note, care should be taken when altering aptamer sequences because alterations to the sequence can detrimentally affect target-binding ability (3).

3.4. Function in Complex Media

One of the most compelling attributes of E-AB sensors is the ability to function in complex media. This attribute is a result of specific aptamer-target interactions and selective electrochemical detection of specific redox markers. To date, aptamer-based sensors have been tested in a variety of complex media, including foodstuffs (55), undiluted serum (1, 4, 7), saliva (18, 55), whole blood (8, 50), and in the circulating blood of living animals measured in real time (17). Although detection can be performed, complications can still arise from nonspecific binding, as described in a recent report by Ferguson et al. (17) in which a sensing device is coupled with a microfluidic filter to perform in vivo detection (see below). Conversely, E-AB sensors fabricated with RNA aptamers are less able to function in complex media as a result of the inherent instability of RNA and susceptibility to nuclease degradation. RNA-based sensors will function in serum only after the serum has been filtered (using a 3,000 molecular weight cutoff filter) or treated with an RNase inhibitor. For example, Ferapontova et al. (16) compared RNA E-AB sensor function in buffer and RNase inhibitor-treated serum: They found RNA sensors did not function at all in untreated serum, further indicating nucleases are the main cause of RNA sensor instability (7, 16).

4. ILLUSTRATIVE EXAMPLES OF APTAMER-BASED SENSING

The growing analytical detection capabilities of E-AB sensors are a direct consequence of their sensitive signaling mechanism as well as the specific recognition abilities of aptamers. Recent advances in the field have shown the significant utility of these unique attributes of structure-switching E-AB sensors. Though not all-encompassing, the illustrative reports we discuss below highlight some of the major breakthroughs achieved thus far in the field, which attest to the analytical promise of this class of sensor.

4.1. Ion and Small-Molecule Detection

One advantage of conformation-switching aptamers is realized in the detection of low-molecular-weight targets, including inorganic ions and small molecules. Radi & O'Sullivan (56) first demonstrated a conformation-switching aptamer sensor for the detection of potassium (K^+) ions via the use of guanine-rich (G-rich) DNA aptamers appended to a gold electrode surface. The G-quartet structure is particularly well suited to recognize monovalent cations, specifically K^+ ions (56). The G-rich aptamers undergo recognition-induced conformation changes that promote conversion of loose random-coil sequences into a more compact G-quadruplex form. This method was highly selective for K^+ ions when tested against other mono- or divalent cations (e.g., Na^+, Mg^{2+}, Ca^{2+}) and achieved a limit of detection of ~0.015 mM (56). As a point of comparison for sensor performance, state-of-the-art all-solid-state ion selective electrodes are capable of limits of detection for K^+ in the nanomolar range (57–59), which far exceeds the abilities of the E-AB sensor analog. However, the detection limit and dynamic range of the E-AB sensor for K^+ is amenable to physiological concentrations (low mM) of potassium. In addition, the study by Radi & O'Sullivan validates the potential of coupling nucleic acid structure-switching for the development of E-AB sensors to detect small targets with good sensitivity and selectivity, however, their study also highlights an issue that may plague E-AB sensors—structural sensitivity to ion composition—because several DNA and RNA structural motifs rely on a specific ion composition. Examples include the dependence of the G-quadruplex motif on K^+ ions (51) as well as the K-turn (kink turn) motif on Mg^{2+} ions (60).

E-AB sensors have made excellent progress beyond the benchtop in the detection of small molecules. Notable publications from Baker et al. (18), Zayats et al. (61), Wu et al. (62), and Zhang et al. (63) demonstrate the utility of these sensors in the detection of small molecules, such as purine nucleosides (61–63) and small drugs (18). As mentioned above, work by the groups of Plaxco and Soh (17) introduced rapid, reusable, and label-free electrochemical detection of circulating therapeutic agents directly into the flowing blood of a living animal. The microfluidic-based electrochemical sensing platform, termed as MEDIC (microfluidic electrochemical detector for in vivo continuous monitoring), detected therapeutic in vivo concentrations of doxorubicin and kanamycin in live rats and in human whole blood with high sensitivity and subminute temporal resolution (17). As a point of comparison, the in vivo electrochemical detection of catechol amines at carbon fiber microelectrodes offer ms time resolution, but this method can only be used to detect molecules that have intrinsic electrochemical activity (64). To expand the scope of targets that can be measured in vivo to nonelectrochemically active molecules, several reports have investigated the use of enzyme-modified electrodes. For example, a report by Sombers and coworkers demonstrated in vivo detection of glucose with a low μM detection limit and ~100 ms time resolution (65). The example reported by the groups of Plaxco and Soh represents a clear indication of the translational abilities of E-AB sensors and is the first demonstration of in vivo detection abilities of non-electrochemically active small molecules with comparable analytical abilities to that of state-of-the-art enzyme-modified electrodes. A clear advantage of the E-AB

platform is the potential ability to artificially generate aptamers for virtually any target expanding beyond the scope of of targets with amenable enzymatic reactions.

4.2. Protein Detection

Proteins are yet another type of target successfully studied via structure-switching E-AB sensors. For example, the groups of Plaxco, Heeger, and Revzin each reported a general electrochemical-sensing platform for the detection of the proteins thrombin (14), platelet-derived growth factor (1), interferon gamma (66), and botulism toxin (52) in buffer and in serum. In the presence of the target proteins, the methylene blue–tagged DNA aptamers undergo target-induced conformational changes from partially unfolded states to more rigid folded states and/or vice versa, which alters the efficiency of the electron transfer between the methylene blue redox molecule and the gold surface. In some cases, notably the detection of platelet-derived growth factor, Lai et al. (1) report a limit of detection of 50 pM. By comparison, enzyme-linked immunosorbent assays (the gold standard for protein detection) for the same target boast low pM detection thresholds (67; in this reference a DNA ligation assay achieves zM detection of the same protein). While the E-AB detection limit is not as low, the operational convenience of a one-step E-AB sensor should be noted in comparison to the multiple step, equipment intensive enzyme-linked immunosorbent assay. Interestingly, as mentioned above, the Revzin group (35, 68, 69) introduced a way to carry out simultaneous, multiplexed detection of cytokines (tumor necrosis factor alpha, interferon gamma, and transforming growth factor β1) via fabrication of micropatterned gold electrode arrays functionalized with redox-active DNA aptamers specific for their respective targets and integration with a microfluidic device. Once again, the detection limit of the reported aptamer sensors (∼10 ng/ml) does not match that of the gold standard enzyme-linked immunosorbent assay (∼15 pg/ml) (70), however the ability to perform such detection in near real time as the target is released from cells demonstrates the analytical capabilities of the E-AB sensor approach. This emerging microfluidic-based sensing approach that utilizes the specific recognition mechanism of structure-switching E-AB sensors offers advantages of rapid, simultaneous, sensitive, and highly specific detection of immune cell-secreted cytokines.

These studies demonstrate the tunability and highly flexible sensing capabilities of structure-switching E-AB sensors that make these sensors adaptable to the development of transportable sensing devices. These reports also compellingly demonstrate the powerful sensing abilities of this class of sensor and, thus, may very well present a means to detect a broader range of targets in vitro and particularly in vivo.

5. ALTERNATIVE STRATEGIES: NANOPORE-BASED SENSING

Integration of specific aptamers with single-molecule detection techniques, particularly stochastic nanopore-based sensing, is now being explored as an alternative strategy to further improve sensitivity and detection limit. Stochastic nanopore sensing has emerged as a powerful resistive-pulse, single-molecule detection technology that measures the electrical current carried by ions flowing through a resistive nanopore. Single-binding events in the nanopore cause an increase in resistance that impedes ionic current flow and that can readily be measured and used to identify and quantify target analytes (71–73). Termed aptamer-based nanopores, studies to date demonstrate the detection of various targets such as proteins (74) and biomarkers (75, 76). For example, Rotem et al. (74) demonstrated nanomolar sensitivity of an aptamer-based nanopore sensor via the utility of staphylococcal α-hemolysin modified with a 15-mer DNA aptamer that specifically binds thrombin. In this approach, binding of thrombin to the aptamer hybridized to the α-hemolysinpore produced a cation-stabilized quadruplex that resulted in a modulation

in the ionic current flowing through the pore, allowing sensitive and specific quantification of thrombin in the nanomolar concentration range (20–350 nM) (74).

6. PERSPECTIVES: CHALLENGES OF E-AB SENSORS

Although structure-switching E-AB sensors hold a lot of promise as a detection strategy, there are several challenges that need to be considered when designing and employing new sensors.

6.1. Aptamer Performance Depends on Environmental Factors

An inherent limitation to using biomolecules as a recognition element, such as nucleic acids, is that structure and function depend on environmental factors such as pH, temperature, and ionic strength. In the body, these factors are tightly regulated homeostatically; however, on the bench or in the field, sensor response can be altered based on changes in environmental conditions. Cho et al. (77) directly address these caveats by providing a list of suggested standards when working with and publishing work using aptamers. The authors cite buffer conditions and temperature, among others, as important factors that need to be considered when working with aptamer sequences. A clear example of matrix effects is seen with an E-AB sensor fabricated with the thrombin binding aptamer (14). The thrombin binding aptamer forms a G-quadruplex structure, which requires potassium ions to fold to bind an exo binding site on human α-thrombin. Xiao et al. (78) investigated the dependence of signal change of thrombin E-AB sensors on the ionic strength and composition. They determined that at a high ionic strength (300-mM Tris base, 420-mM NaCl, 60-mM KCl, and 60-mM $MgCl_2$) the apparent binding affinity of an E-AB sensor for thrombin is 50 nM. Conversely, at low ionic strength, without the presence of potassium (100-mM Tris base), the sensor exhibits an apparent binding affinity of 21 nM with an increase in sensitivity as well (78). Without potassium, the aptamer is unfolded and thus likely exhibits a larger conformation change in the presence of thrombin, which leads to better sensitivity. There are several other reports that address the affects of pH and temperature on nucleic acid–based sensors (79, 80). Because matrix effects can affect the performance of a sensor, it is prudent to calibrate sensors in the matrix in which they will be employed. In addition to environmental conditions, the performance of a given aptamer sequence is dramatically altered as a result of the signal transduction methodology employed. A study recently published by McKeague et al. (81) highlights inconsistencies in quantification of aptamer binding parameters resulting from the different assays used to perform the characterization.

6.2. Improving Aptamer Selection

The performance of E-AB sensors is ultimately linked to the quality of the aptamer that is used to fabricate the sensor. Whereas protein-binding aptamers can be extremely specific, aptamers selected for small-molecule binding targets, with only a few exceptions, often lack specificity. For example, protein-binding aptamers including thrombin, interferon gamma, and tumor necrosis factor alpha exemplify target specificity in complex media and when challenged by similar proteins (8, 14, 68). In contrast, the aminoglycoside RNA aptamer will bind several aminoglycoside antibiotics, including tobramycin, kanamycin, neomycin B, gentamycin C, erythromycin, and tobramycin analogs (54). In addition, the cocaine aptamer will bind cocaine, ecgonine methyl ester, lidocaine, and procaine (82). There are counter examples such as RNA theophylline aptamer that binds theophylline with a 500-fold better affinity than caffeine, even though the targets differ by

only a single methyl group (16). As selection procedures improve, the field will greatly benefit from increased specificity and affinity, particularly for low-molecular-weight targets.

6.3. Signal Amplification

The signaling of E-AB sensors is currently limited to only a handful of demonstrated redox markers that can provide approximately one to two electrons worth of charge at most. This limitation in total charge amount ultimately limits the sensitivity and limit of detection of structure-switching aptamer-based sensors. This signaling limitation can be dramatically improved by adding a signal amplification technique that regenerates the redox molecule for amplified currents. Although there are a several of examples of amplification coupled with aptamer recognition (83–86), these examples eliminate one of the most compelling attributes of E-AB sensors—their reagentless nature. An even more difficult task is to apply the amplification to one of the two sensor states—target bound or unbound. We postulate that the introduction of signal amplification that retains the reagentless nature of E-AB sensors would be a major breakthrough in this class of promising biosensors.

6.4. Electrode Miniaturization

Coupling E-AB sensors to micro- and nanoelectrodes may bring the promising attributes of small electrodes—low IR drop, small background capacitive charging current, rapid steady-state equilibration, high current density, and minimal sample requirement (87)—to aptamer recognition to further expand potential sensor applications. These advantages open up E-AB sensor applications to new areas of biological and chemical sensing (5, 88), such as scanning electrochemical microscopy for spatially resolved measurements (89). Furthermore, miniaturization of electrodes allows their integration with devices for minimally invasive in vivo measurements and point-of-care diagnosis. This transition, however, has met many challenges, including limited current signal resulting from the small size and low number of aptamers on the sensor surface. Liu et al. (5) reported the first reversible and reproducible use of microelectrodes for E-AB sensing to detect adenosine triphosphate and tobramycin quantification directly in 100% undiluted serum. This report used deposition of gold nanoparticles to overcome the inherently low signal-to-noise ratio. The introduction of an amplification technique would greatly facilitate the transition to small electrodes.

7. SUMMARY

Advances in the field of structure-switching E-AB have continued to expand over the past 10 years. The ability to select aptamers for virtually any target analyte coupled with the reagentless detection abilities of E-AB sensors make these sensors appealing in a broad range of applications. In this review, we cover several of the important aspects of E-AB sensor design, fabrication, and use. We also highlight several illustrations of the utility of E-AB sensors in the direct detection of target molecules in complex environments, including in vivo measurements, owing to their reagentless, reusable, and specific nature. Although E-AB sensors show promise for the future of analytical detection, there are several hurdles that impede translational progress. However, it is likely that several of these hurdles will be overcome in the coming years.

The translation of E-AB sensors into areas such as clinical diagnostics and field-portable devices is a compelling frontier for this class of reagentless sensor. The field of E-AB sensors will continue to grow with the benefit of ever-improving aptamer selection strategies that will further expand the range of accessible targets. New selection strategies to improve specificity of target-aptamer interactions are crucial to this progress. The coupling of small electrode-based sensors

can expand the utility of aptamer sensors to enable the study of new realms of biological processes and to provide minimally invasive tools for the biomedical field. Progress in these areas will also benefit from the introduction of a signal amplification strategy that keeps the reagentless nature of E-AB sensors. In summary, E-AB sensors are poised to impact analytical chemistry beyond the well-controlled laboratory benchtop. Investigators are at the brink of exciting new demonstrated applications of E-AB sensors.

DISCLOSURE STATEMENT

The authors are not aware of any affiliations, memberships, funding, or financial holdings that might be perceived as affecting the objectivity of this review.

ACKNOWLEDGMENTS

The authors greatly acknowledge support from the National Institute of Mental Health of the National Institutes of Health under award number 1R21MH101692 (R.J.W.); the National Institute of General Medical Sciences of the National Institutes of Health under award number T32GM066706 (K.S.R., F.C.M.); and a CBI grant from the Department of Chemistry and Biochemistry, University of Maryland, Baltimore County. The content is solely the responsibility of the authors and does not necessarily represent the official views of the National Institutes of Health.

LITERATURE CITED

1. Lai RY, Plaxco KW, Heeger AJ. 2007. Aptamer-based electrochemical detection of picomolar platelet-derived growth factor directly in blood serum. *Anal. Chem.* 79:229–33
2. White RJ, Phares N, Lubin AA, Xiao Y, Plaxco KW. 2008. Optimization of electrochemical aptamer-based sensors via optimization of probe packing density and surface chemistry. *Langmuir* 24:10513–18
3. Schoukroun-Barnes L, White R. 2015. Rationally designing aptamer sequences with reduced affinity for controlled sensor performance. *Sensors* 15:7754–67
4. Swensen JS, Xiao Y, Ferguson BS, Lubin AA, Lai RY, et al. 2009. Continuous, real-time monitoring of cocaine in undiluted blood serum via a microfluidic, electrochemical aptamer-based sensor. *J. Am. Chem. Soc.* 131:4262–66
5. Liu J, Wagan S, Davila Morris M, Taylor J, White RJ. 2014. Achieving reproducible performance of electrochemical, folding aptamer-based sensors on microelectrodes: challenges and prospects. *Anal. Chem.* 86:11417–24
6. Porchetta A, Vallée-Bélisle A, Plaxco KW, Ricci F. 2012. Using distal-site mutations and allosteric inhibition to tune, extend, and narrow the useful dynamic range of aptamer-based sensors. *J. Am. Chem. Soc.* 134:20601–4
7. Rowe AA, Miller EA, Plaxco KW. 2010. Reagentless measurement of aminoglycoside antibiotics in blood serum via an electrochemical, ribonucleic acid aptamer-based biosensor. *Anal. Chem.* 82:7090–95
8. Liu Y, Zhou Q, Revzin A. 2013. An aptasensor for electrochemical detection of tumor necrosis factor in human blood. *Analyst* 138:4321–26
9. Kang D, Zuo X, Yang R, Xia F, Plaxco KW, White RJ. 2009. Comparing the properties of electrochemical-based DNA sensors employing different redox tags. *Anal. Chem.* 81:9109–13
10. Ferapontova EE, Gothelf K V. 2009. Effect of serum on an RNA aptamer-based electrochemical sensor for theophylline. *Langmuir* 25:4279–83
11. Willner I, Zayats M. 2007. Electronic aptamer-based sensors. *Angew. Chem. Int. Ed.* 46:6408–18
12. Song S, Wang L, Li J, Fan C, Zhao J. 2008. Aptamer-based biosensors. *Trends Anal. Chem.* 27:108–17
13. Liu J, Morris MD, Macazo FC, Schoukroun-Barnes LR, White RJ. 2014. The current and future role of aptamers in electroanalysis. *J. Electrochem. Soc.* 161:H301–13

14. Xiao Y, Lubin AA, Heeger AJ, Plaxco KW. 2005. Label-free electronic detection of thrombin in blood serum by using an aptamer-based sensor. *Angew. Chem. Int. Ed.* 44:5456–59
15. Rajendran M, Ellington AD. 2003. In vitro selection of molecular beacons. *Nucleic Acids Res.* 31:5700–13
16. Ferapontova EE, Olsen EM, Gothelf KV. 2008. An RNA aptamer-based electrochemical biosensor for detection of theophylline in serum. *J. Am. Chem. Soc.* 130:4256–58
17. Ferguson BS, Hoggarth DA, Maliniak D, Ploense K, White RJ, et al. 2013. Real-time, aptamer-based tracking of circulating therapeutic agents in living animals. *Sci. Transl. Med.* 5:213ra165
18. Baker BR, Lai RY, Wood MS, Doctor EH, Heeger AJ, Plaxco KW. 2006. An electronic, aptamer-based small-molecule sensor for the rapid, label-free detection of cocaine in adulterated samples and biological fluids. *J. Am. Chem. Soc.* 128:3138–39
19. Levicky R, Herne TM, Tarlov MJ, Satija SK. 1998. Using self-assembly to control the structure of DNA monolayers on gold: a neutron reflectivity study. *J. Am. Chem. Soc.* 120:9787–92
20. Josephs EA, Ye T. 2013. Nanoscale spatial distribution of thiolated DNA on model nucleic acid sensor surfaces. *ACS Nano*. 7:3653–60
21. Macazo FC, Karpel RL, White RJ. 2015. Monitoring cooperative binding using electrochemical DNA-based sensors. *Langmuir* 31:868–75
22. Lai RY, Seferos DS, Heeger AJ, Bazan GC, Plaxco KW. 2006. Comparison of the signaling and stability of electrochemical DNA sensors fabricated from 6- or 11-carbon self-assembled monolayers. *Langmuir* 22:10796–800
23. Ulman A. 1996. Formation and structure of self-assembled monolayers. *Chem. Rev.* 96:1533–54
24. Ricci F, Zari N, Caprio F, Recine S, Amine A, et al. 2009. Surface chemistry effects on the performance of an electrochemical DNA sensor. *Bioelectrochemistry* 76:208–13
25. Ricci F, Lai RY, Heeger AJ, Plaxco KW, Sumner JJ. 2007. Effect of molecular crowding on the response of an electrochemical DNA sensor. *Langmuir* 23:6827–34
26. Steel AB, Levicky RL, Herne TM, Tarlov MJ. 2000. Immobilization of nucleic acids at solid surfaces: effect of oligonucleotide length on layer assembly. *Biophys. J.* 79:975–81
27. Xiao Y, Lai RY, Plaxco KW. 2007. Preparation of electrode-immobilized, redox-modified oligonucleotides for electrochemical DNA and aptamer-based sensing. *Nat. Protoc.* 2:2875–80
28. Schoukroun-Barnes LR, Wagan S, White RJ. 2014. Enhancing the analytical performance of electrochemical RNA aptamer-based sensors for sensitive detection of aminoglycoside antibiotics. *Anal. Chem.* 86:1131–37
29. Ferapontova EE, Gothelf KV. 2009. Optimization of the electrochemical RNA-aptamer based biosensor for theophylline by using a methylene blue redox label. *Electroanalysis* 21:1261–66
30. Prins R, Korswagen AR, Kortbeek AGTG. 1972. Decomposition of the ferricenium cation by nucleophilic reagents. *J. Organomet. Chem.* 39:335–44
31. Han SW, Se H, Chung K, Kim K. 2000. Electrochemical and vibrational spectroscopic characterization of self-assembled monolayers of 1,1′-disubstituted ferrocene derivatives on gold. *Langmuir* 16:9493–500
32. Zhang S, Zhou G, Xu X, Cao L, Liang G, et al. 2011. Development of an electrochemical aptamer-based sensor with a sensitive Fe_3O_4 nanopaticle-redox tag for reagentless protein detection. *Electrochem. Commun.* 13:928–31
33. Chang AL, McKeague M, Liang JC, Smolke CD. 2014. Kinetic and equilibrium binding characterization of aptamers to small molecules using a label-free, sensitive, and scalable platform. *Anal. Chem.* 86:3273–78
34. Latham MP, Zimmermann GR, Pardi A. 2009. NMR chemical exchange as a probe for ligand-binding kinetics in a theophylline-binding RNA aptamer. *J. Am. Chem. Soc. Commun.* 131:5052–53
35. Liu Y, Liu Y, Matharu Z, Rahimian A, Revzin A. 2015. Detecting multiple cell-secreted cytokines from the same aptamer-functionalized electrode. *Biosens. Bioelectron.* 64:43–50
36. Pheeney CG, Barton JK. 2012. DNA electrochemistry with tethered methylene blue. *Langmuir* 2:7063–70
37. Uzawa T, Cheng RR, White RJ, Makarov DE, Plaxco KW. 2010. A mechanistic study of electron transfer from the distal termini of electrode-bound, single-stranded DNAs. *J. Am. Chem. Soc.* 132:16120–26
38. Huang K, White RJ. 2013. Random walk on a leash: a simple single-molecule diffusion model for surface-tethered redox molecules with flexible linkers. *J. Am. Chem. Soc.* 135:12808–17
39. Farjami E, Campos R, Ferapontova EE. 2012. Effect of the DNA end of tethering to electrodes on electron transfer in methylene blue-labeled DNA duplexes. *Langmuir* 28:16218–26

40. Anne A, Bouchardon A, Moiroux J. 2003. 3′-ferrocene-labeled oligonucleotide chains end-tethered to gold electrode surfaces: novel model systems for exploring flexibility of short DNA using cyclic voltammetry. *J. Am. Chem. Soc.* 125:1112–13
41. Anne A, Demaille C. 2006. Dynamics of electron transport by elastic bending of short DNA duplexes. Experimental study and quantitative modeling of the cyclic voltammetric behavior of 3′-ferrocenyl DNA end-grafted on gold. *J. Am. Chem. Soc.* 128:542–57
42. Steel AB, Herne TM, Tarlov MJ. 1998. Electrochemical quantitation of DNA immobilized on gold. *Anal. Chem.* 70:4670–77
43. Esteban B, Watkins HM, Pingarro JM, Plaxco KW, Palleschi G, Ricci F. 2013. Determinants of the detection limit and specificity of surface-based biosensors. *Anal. Chem.* 85:6593–97
44. Schoukroun-Barnes LR, Glaser EP, White RJ. 2015. Heterogeneous electrochemical aptamer-based sensor surfaces for controlled sensor response. *Langmuir* 31:6563–69
45. White RJ, Plaxco KW. 2010. Exploiting binding-induced changes in probe flexibility for the optimization of electrochemical biosensors. *Anal. Chem.* 82:73–76
46. Ricci F, Lai RY, Plaxco KW. 2007. Linear, redox modified DNA probes as electrochemical DNA sensors. *Chem. Commun.* 2007:3768–70
47. Zuker M, Jacobson AB. 1998. Using reliability information to annotate RNA secondary structures. Using reliability information to annotate RNA secondary structures. *RNA* 4:669–79
48. Zuker M. 2003. Mfold web server for nucleic acid folding and hybridization prediction. *Nucleic Acids Res.* 31:3406–15
49. White RJ, Rowe AA, Plaxco KW. 2010. Re-engineeing aptamers to support reagentless, self-reporting electrochemical sensors. *Analyst* 135:589–94
50. White RJ, Plaxco KW. 2009. Engineering new aptamer geometries for electrochemical aptamer-based sensors. *Proc. SPIE Int. Soc. Opt. Eng.* 7321:732105
51. Catherine AT, Shishido SN, Robbins-Welty GA, Diegelman-Parente A. 2014. Rational design of a structure-switching DNA aptamer for potassium ions. *FEBS Open Bio* 4:788–95
52. Fetter L, Richards J, Daniel J, Roon L, Rowland TJ, Bonham AJ. 2015. Electrochemical aptamer scaffold biosensors for detection of botulism and ricin toxins. *Chem. Commun.* 51:15137–40
53. Jiang L, Patel D. 1998. Solution structure of the tobramycin-RNA aptamer complex. *Nat. Struct. Biol.* 5:769–74
54. Wang Y, Rando RR. 1995. Specific binding of aminoglycoside antibiotics to RNA. *Chem. Biol.* 2:281–90
55. Lubin AA, Lai RY, Baker BR, Heeger AJ, Plaxco KW. 2006. Sequence-specific, electronic detection of oligonucleotides in blood, soil, and foodstuffs with the reagentless, reusable E-DNA sensor. *Anal. Chem.* 78:5671–77
56. Radi A-E, O'Sullivan CK. 2006. Aptamer conformational switch as sensitive electrochemical biosensor for potassium ion recognition. *Chem. Commun.* 2006:3432–34
57. Hu J, Stein A, Bühlmann P. 2016. Rational design of all-solid-state ion-selective electrodes and reference electrodes. *Trends Anal. Chem.* 76:102–14
58. Chumbimuni-Torres KY, Rubinova N, Radu A, Kubota LT, Bakker E. 2006. Solid contact potentiometric sensors for trace level measurements. *Anal. Chem.* 78:1318–22
59. Mensah ST, Gonzalez Y, Calvo-Marzal P, Chumbimuni-Torres KY. 2014. Nanomolar detection limits of Cd^{2+}, Ag^{+}, and K^{+} using paper-strip ion-selective electrodes. *Anal. Chem.* 86:7269–73
60. Blouin S, Lafontaine DA. 2007. A loop-loop interaction and a K-turn motif located in the lysine aptamer domain are important for the riboswitch gene regulation control. *RNA* 13:1256–67
61. Zayats M, Huang Y, Gill R, Ma CA, Willner I. 2006. Label-free and reagentless aptamer-based sensors for small molecules. *J. Am. Chem. Soc.* 128:13666–67
62. Wu Z-S, Guo M-M, Zhang S-B, Chen C-R, Jiang J-H, et al. 2007. Reusable electrochemical sensing platform for highly sensitive detection of small molecules based on structure-switching signaling aptamers. *Anal. Chem.* 79:2933–39
63. Zhang S, Xia J, Li X. 2008. Electrochemical biosensor for detection of adenosine based on structure-switching aptamer and amplification with reporter probe DNA modified Au nanoparticles. *Anal. Chem.* 80:8382–88

64. Bucher ES, Wightman RM. 2015. Electrochemical analysis of neurotransmitters. *Ann. Rev. Anal. Chem.* 8:239–61
65. Lugo-Morales LZ, Loziuk PL, Corder AK, Toups JV, Roberts JG et al. 2013. Enzyme-modified carbon-fiber microelectrode for the quantification of dynamic fluctuations of nonelectroactive analytes using fast-scan cyclic voltammatery. *Anal. Chem.* 85:8780–86
66. Liu Y, Tuleouva N, Ramanculov E, Revzin A. 2010. Aptamer-based electrochemical biosensor for interferon gamma detection. *Anal. Chem.* 82:8131–36
67. Fredriksson S, Gullberg M, Jarvius J, Olsson C, Pietras K, et al. 2002. Protein detection using proximity-dependent DNA ligation assays. *Nature Biotech.* 20:473–77
68. Liu Y, Kwa T, Revzin A. 2012. Simultaneous detection of cell-secreted TNF-α and IFN-γ using micropatterned aptamer-modified electrodes. *Biomaterials* 33:7347–55
69. Matharu Z, Patel D, Gao Y, Haque A, Zhou Q, Revzin A. 2014. Detecting transforming growth factor-β release from liver cells using an aptasensor integrated with microfluidics. *Anal. Chem.* 86:8865–72
70. Connel TG, Curtis N, Ranganathan SC, Buttery JP. 2006. Performance of a whole blood interferon gamma assay for detecting latent infenction with *Mycobacterium tuberculosis* in children. *Thorax* 61:616–20
71. Bayley H, Cremer PS. 2001. Stochastic sensors inspiored by biology. *Nature* 413:226–30
72. Bayley H, Martin CR. 2000. Resistive-pulse sensing-from microbes to molecules. *Chem. Rev.* 100:2575–94
73. Macazo FC, White RJ. 2014. Monitoring charge flux to quantify unusual ligand-induced ion channel activity for use in biological nanopore-based sensors. *Anal. Chem.* 86:5519–25
74. Rotem D, Jayasinghe L, Salichou M, Bayley H. 2012. Protein detection by nanopores equipped with aptamers. *J. Am. Chem. Soc.* 134:2781–87
75. Li T, Liu L, Li Y, Xie J, Wu H-C. 2015. A universal strategy for aptamer-based nanopore sensing through host-guest interactions inside α-hemolysin. *Angew. Chem. Int. Ed.* 54:7568–71
76. Zhang L, Zhang K, Liu G, Liu M, Liu Y, Li J. 2015. Rapid and label-free nanopore proximity bioassay for platelet-derived growth factor detection. *Anal. Chem.* 87:5677–82
77. Cho EJ, Lee J-W, Ellington AD. 2009. Applications of aptamers as sensors. *Annu. Rev. Anal. Chem.* 2:241–64
78. Xiao Y, Uzawa T, White RJ, DeMartini D, Plaxco KW. 2009. On the signaling of electrochemical aptamer-based sensors: collision- and folding-based mechanisms. *Electroanalysis* 21:1267–71
79. Mao Y, Luo C, Ouyang Q. 2003. Studies of temperature-dependent electronic transduction on DNA hairpin loop sensor. *Nucleic Acids Res.* 31:e108
80. Hianik T, Ostatná V, Sonlajtnerova M, Grman I. 2007. Influence of ionic strength, pH and aptamer configuration for binding affinity to thrombin. *Bioelectrochemistry* 70:127–33
81. McKeague M, De Girolamo A, Valenzano S, Pascale M, Ruscito A, et al. 2015. Comprehensive analytical comparison of strategies used for small molecule aptamer evaluation. *Anal. Chem.* 87:8608–12
82. Stojanovic MN, de Prada P, Landry DW, Prada P De, Landry DW. 2001. Aptamer-based folding fluorescent sensor for cocaine. *J. Am. Chem. Soc.* 123:4928–31
83. Zuo X, Xiao Y, Plaxco KW. 2009. High specificity, electrochemical sandwich assays based on single aptamer sequences and suitable for the direct detection of small-molecule targets in blood and other complex matrices. *J. Am. Chem. Soc.* 131:6944–45
84. Zuo X, Song S, Zhang J, Pan D, Wang L, Fan C. 2007. A target-responsive electrochemical aptamer switch (TREAS) for reagentless detection of nanomolar ATP. *J. Am. Chem. Soc.* 129:1042–43
85. Ikebukuro K, Kiyohara C, Sode K. 2005. Novel electrochemical sensor system for protein using the aptamers in sandwich manner. *Biosens. Bioelectron.* 20:2168–72
86. Miao P, Tang Y, Wang B, Han K, Chen X, Sun H. 2014. An aptasensor for detection of potassium ions based on $RecJ_f$ exonuclease mediated signal amplification. *Analyst* 139:5695–99
87. Cox JT, Zhang B. 2012. Nanoelectrodes: recent advances and new directions. *Annu. Rev. Anal. Chem.* 5:253–72
88. Wang T, Viennois E, Merlin D, Wang G. 2015. Microelectrode miRNA sensors enabled by enzymeless electrochemical signal amplification. *Anal. Chem.* 87:8173–80
89. Hu K, Gao Y, Wang Y, Yu Y, Zhao X, et al. 2013. Platinized carbon nanoelectrodes as potentiometric and amperometric SECM probes. *J. Solid State Electrochem.* 17:2971–77